

Copper(II) 12-Metallacrown-4: Synthesis, Structure, Ligand Variability, and Solution Dynamics in the 12-MC-4 Structural Motif

Brian R. Gibney, Dimitris P. Kessissoglou, Jeff W. Kampf, and Vincent L. Pecoraro*

Willard H. Dow Laboratories, Department of Chemistry, The University of Michigan, Ann Arbor, Michigan 48109-1055

Received February 15, 1994[⊗]

An important goal for generalizing the metallacrown analogy was to prepare metallacrowns with divalent ring metals using di- and trianionic supporting organic ligands that retain a high yield synthesis for a predicted metallacrown structural motif. This goal has been achieved with Cu(II) using anthranilic hydroxamic acid, 2-pyridylacetohydroxamic acid, 3-hydroxy-2-naphthohydroxamic acid, salicylhydroxamic acid, 5-deuterio- and 3,5 dideuterio-salicylhydroxamic acid, 4-hydroxysalicylhydroxamic acid, 4-methylsalicylhydroxamic acid, 5-hydroxysalicylhydroxamic acid, 5-methoxysalicylhydroxamic acid and 5-butylsalicylhydroxamic acid. These organic ligands vary not only the organic periphery but also the metal coordination donor set. Each forms the generalized $[\text{Cu}^{\text{II}}(12\text{-MC}_{\text{Cu}(\text{II})\text{N}(\text{ligand})\text{-4}})]$ structure in one-step, high yield syntheses. The dianionic ligands (e.g. anthranilic hydroxamic acid) demonstrate that neutral metallacrown rings with divalent ring metals may be synthesized. The trianionic ligands (e.g. salicylhydroxamic acid) provide the first formally charged metallacrown rings demonstrating that the accumulation of charge does not hinder metallacrown formation. Appending hydroxy, alkyl, and alkyloxy functional groups to the $[\text{Cu}^{\text{II}}(12\text{-MC-4})]$'s demonstrate in principle that incorporation of functionalities potentially capable of forming mesogenic phases or binding to clean metal surfaces can be accomplished. A variety of analytical techniques, i.e. UV-vis, ESI-MS, FAB-MS, and solution magnetic susceptibility measurements, were employed to probe the solution integrity and dynamics of the $[\text{Cu}^{\text{II}}(12\text{-MC-4})]$'s. These studies allow us to conclude that all of the copper metallacrowns presented retain their structure in solution. Additionally, UV-vis titrations demonstrate the $[\text{Cu}^{\text{II}}(12\text{-MC-4})]$'s are stable in DMF even in the presence of excess acetate ion or ligand. The solution dynamics of the $[\text{Cu}^{\text{II}}(12\text{-MC-4})]$ system was probed using electrospray ionization mass spectrometry and ¹H NMR. These studies revealed that the copper(II) 12-metallacrown-4's are inert to ligand exchange. Variable temperature magnetic susceptibility measurements show weak antiferromagnetic coupling between the copper(II) ions in the metallacrown which results in an $S = 1/2$ ground state, i.e. $\mu_{\text{eff}} \approx 1.73 \mu_{\text{B}}$ per metallacrown at 4 K. The solution and solid state magnetic susceptibilities at 300 K are comparable, thus providing additional evidence for metallacrown solution integrity. The totality of evidence from UV-vis, ESI-MS and FAB-MS, ¹H NMR, solution magnetic susceptibility measurements, and EPR support the conclusion that copper(II) metallacrowns retain their structure in solution. Thus, metallacrowns represent a convenient high yield entry into stable, paramagnetic, polymetallic species with surface areas $\approx 2.0 \text{ nm}^2$ ($1.4 \text{ nm} \times 1.4 \text{ nm}$). The complex $[\text{Cu}^{\text{II}}(12\text{-MC}_{\text{Cu}(\text{II})\text{N}(\text{anha})\text{-4}})](\text{ClO}_4)_2 \cdot 3\text{MeOH}$, **1b**, $\text{Cu}_5\text{C}_{31.75}\text{H}_{40}\text{N}_8\text{O}_{20.25}\text{Cl}_2$, 1245 g/mol, crystallizes in the triclinic space group $P\bar{1}$ (No. 2), with $a = 11.077(2) \text{ \AA}$, $b = 12.294(2) \text{ \AA}$, $c = 17.272(4) \text{ \AA}$, $\alpha = 110.29(2)^\circ$, $\beta = 96.05(2)^\circ$, $\gamma = 96.27(1)^\circ$, $V = 2166.9(7) \text{ \AA}^3$, and $Z = 2$. The structure was solved and refined by full-matrix least-squares methods down to $R = 0.059$ and $R_w = 0.082$ for 9842 independent reflections with $5^\circ < 2\theta < 60^\circ$ and $(F_o) \geq 3\sigma(F)$. X-ray parameters for $(\text{TEA})_2[\text{Cu}^{\text{II}}(12\text{-MC}_{\text{Cu}(\text{II})\text{N}(\text{nha})\text{-4}})] \cdot \text{DMF}$, **3**, $\text{Cu}_5\text{C}_{63}\text{H}_{71}\text{N}_7\text{O}_{13}$, 1452 g/mol; crystal system monoclinic, $C2/c$ (No. 15), $a = 31.600(4) \text{ \AA}$, $b = 8.108(2) \text{ \AA}$, $c = 27.180(4) \text{ \AA}$, $\beta = 102.97(1)^\circ$, $V = 6786(2) \text{ \AA}^3$, $Z = 4$, 16623 data collected with $5^\circ < 2\theta < 55^\circ$, 6986 data with $(F_o) \geq 2\sigma(F)$, $R = 0.0609$, $R_w = 0.0924$. X-ray parameters for $(\text{Na}(15\text{-C-5}))_2[\text{Cu}^{\text{II}}(12\text{-MC}_{\text{Cu}(\text{II})\text{N}(\text{shi})\text{-4}})] \cdot \text{MeOH}$, **4a**, $\text{Na}_2\text{Cu}_5\text{C}_{52.5}\text{H}_{78}\text{N}_4\text{O}_{26.5}$, 1553 g/mol, crystal system monoclinic, $C2/c$ (No. 15), $a = 34.97(1) \text{ \AA}$, $b = 14.350(6) \text{ \AA}$, $c = 29.00(2) \text{ \AA}$, $\beta = 120.30(4)^\circ$, $V = 12563(10) \text{ \AA}^3$, $Z = 8$, 6797 data collected with $5^\circ < 2\theta < 40^\circ$, 3789 data with $(F_o) \geq 4\sigma(F)$, $R = 0.1226$, $R_w = 0.0840$. X-ray parameters for $(\text{TMA})_2[\text{Cu}^{\text{II}}(12\text{-MC}_{\text{Cu}(\text{II})\text{N}(\text{shi})\text{-4}})] \cdot \text{DMF}$, **4b**, $\text{Cu}_5\text{C}_{42}\text{H}_{54}\text{N}_8\text{O}_{14}$, 1212.6 g/mol, crystal system rhombohedral, $R\bar{3}$ (No. 148), $a = b = 33.634(8) \text{ \AA}$, $c = 11.276(2) \text{ \AA}$, $V = 11059(5) \text{ \AA}^3$, $Z = 9$, 13 668 data collected with $5^\circ < 2\theta < 50^\circ$, 4332 unique data refined on F^2 , $wR^2 = 0.1242$, the conventional residual for $F_o \geq 4\sigma(F_o)$ is 0.0423.

The "metallacrown analogy"¹ is a powerful synthetic protocol for the preparation of multinuclear complexes containing moderate valent transition metal ions. Figure 1 illustrates conceptually the structural "analogy" that one may substitute heteroatoms such as transition metals and nitrogen for the methylene carbons of their analogous organic crown ethers.²⁻⁵ The presence of transition metal ions in the metallacrown

linkage, $\text{M}^{\text{x+}}\text{-N-O}$, leads to a class of molecules with features distinct from the simple organic crowns, such as strong visible absorption spectra, redox activity, and magnetism.^{6,7} Metalla-

(3) Pedersen, C. J. *J. Am. Chem. Soc.* **1967**, *89*, 2495.

(4) Pedersen, C. J. *Angew. Chem., Int. Ed. Engl.* **1988**, *27*, 1021.

(5) Lehn, J.-M. *Angew. Chem., Int. Ed. Engl.* **1988**, *27*, 89.

(6) Hiraoka, M. *Crown Ethers and Analogous Compounds*; Elsevier: New York, 1992; Vol. 45, p 485.

(7) Weber, E.; Toner, J. L.; Goldberg, I.; Vögtle, F.; Laidler, D. A.; Stoddart, J. F.; Bartsch, R. A.; Liotta, C. L. *Crown Ethers and Analogs*; John Wiley & Sons: New York, 1989; p 558.

[⊗] Abstract published in *Advance ACS Abstracts*, October 1, 1994.

(1) Lah, M. S.; Pecoraro, V. L. *Comments Inorg. Chem.* **1990**, *11*, 59.

(2) Pedersen, C. J. *J. Am. Chem. Soc.* **1967**, *89*, 7017.

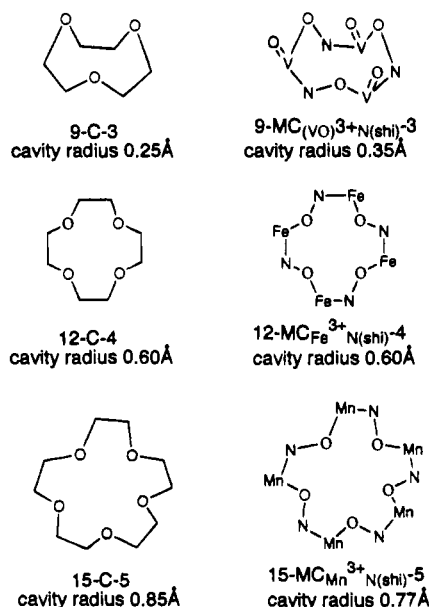


Figure 1. Structures showing the metallacrown analogy utilized as a design concept for the preparation of moderate valent polynuclear transition metal complexes.

crowns have been characterized with V(V)O,^{8,9} Mn(III),^{10–12} Fe(III),^{1,13} Cu(II),¹⁴ and Ga(III)¹⁵ in the ring positions utilizing hydroxamic acid ligands such as salicylhydroxamic acid (H₃-shi)¹ and β -alanine hydroxamic acid (H₂ β -aha).¹⁴ The difference in basicity of the hydroximate oxygen with respect to aliphatic ether oxygens offers the metallacrowns selectivity for encapsulating transition metal ions.¹¹ A wide variety of metal ions, e.g. Na(I),¹¹ Mg(II),¹⁰ Mn(II),^{10,12} and Fe(III),^{1,13} are encapsulated in metallacrown cavities. Furthermore, several structural motifs including 9-MC-3, 12-MC-4, 15-MC-5, and metallacryptates have been prepared.^{1,12,15} The rich coordination chemistry available utilizing the metallacrown analogy is clear when one considers the controlled variability of the composition, structure and physical properties possible with this system.

Cognizant of the limitations of metallacrowns based solely on an shi³⁻ template, we have greatly expanded the types of precursor ligands with the intention of designing organic molecules that will profoundly affect the electronic and physical properties of the metallacrowns. The alterations in ligand donor set coupled with the possibility of appending peripheral architecture allows for rational design of metallacrowns as surface electrode modifiers¹⁶ and metallomesogens.^{17–19} Crucial to these applications is establishing whether one can synthesize metallacrowns of desired structure from organic ligands with

altered donor groups in high yield. We have established this concept using the high valent, early transition element V(V) which forms 9-MC-3 structures.⁹ The report of the [Cu^{II}(12-MC_{Cu(II)N(β -aha)⁻⁴)](ClO₄)₂ utilizing a dianionic ligand with a two nitrogen, two oxygen donor set for the ring metals encouraged an effort to expand this chemistry to lower valent, late transition elements with the 12-MC-4 structural motif.¹⁴ All previously reported metallacrowns have contained rings that are formally neutral with the charges on the resulting metallacrowns being dictated by the encapsulated metal and bridging anion(s). The use of divalent metals such as Cu(II) with trianionic ligands, shi³⁻ and its derivatives, will lead to charged metallacrown rings (e.g., [12-MC_{Cu(II)N(shi)-4}]) should be a tetraanion) that could hinder complex formation.^{20,21}}

Inherent to the future applications of metallacrowns as platforms for supramolecular design is their integrity in solution. Previous studies have established¹⁵ that the metallacryptate retains its structure when dissolved in a variety of solvents and [Cu^{II}(12-MC_{Cu(II)N(β -aha)⁻⁴)](ClO₄)₂ is stable in H₂O between pH 4.5 and 9.0.¹⁴ We have recently shown [9-MC_{V(V)O}N(shi)-3] and [9-MC_{V(V)O}N(nha)-3] to be labile in methanol but inert in acetonitrile under competitive conditions.⁹ Determination of the solution integrity of the [Cu^{II}(12-MC_{Cu(II)N(ligand)⁻⁴)] motif both under noncompetitive and competitive conditions will provide valuable evidence for the solution dynamics of the metallacrowns.}}

Herein, we address a series of points including (a) whether the 12-MC-4 structure type can be obtained with a divalent metal and a multitude of ligands, (b) whether replacement of the phenolate donor with an aryl amine nitrogen or a pyridyl nitrogen affects metallacrown syntheses, (c) whether stable metallacrown rings can be prepared that have formal charge, (d) whether the [Cu^{II}(12-MC_{Cu(II)N(ligand)⁻⁴)] complexes retain the nuclearity that is seen in the solid state in a variety of solvents, and (e) whether copper metallacrowns are stable under ligand competition conditions.}

Experimental Section

Materials. Salicylhydroxamic acid [H₃shi], copper(II) acetate, copper(II) chloride hydrate, copper(II) perchlorate, sodium acetate, potassium acetate, tetramethylammonium acetate, tetraethylammonium acetate, 1,4,7,10,13-pentaoxacyclopentadecane, ethyl-2-amino benzoate,

- (8) Pecoraro, V. L. *Inorg. Chim. Acta* **1989**, *155*, 171.
- (9) Gibney, B. R.; Stemmler, A. J.; Pilotek, S.; Kampf, J. W.; Pecoraro, V. L. *Inorg. Chem.* **1993**, *32*, 6008.
- (10) Lah, M. S.; Pecoraro, V. L. *J. Am. Chem. Soc.* **1989**, *111*, 7258.
- (11) Lah, M. S.; Pecoraro, V. L. *Inorg. Chem.* **1991**, *30*, 878.
- (12) Kessissoglou, D. P.; Kampf, J. W.; Pecoraro, V. L. *Polyhedron* **1994**, *13*, 1379.
- (13) Lah, M. S.; Kirk, M. L.; Hatfield, W.; Pecoraro, V. L. *J. Chem. Soc., Chem. Commun.* **1989**, 1606.
- (14) Kurzak, B.; Farkas, E.; Glowiak, T.; Kozlowski, H. *J. Chem. Soc., Dalton Trans.* **1991**, 163.
- (15) Lah, M. S.; Gibney, B. R.; Tierney, D. L.; Penner-Hahn, J. E.; Pecoraro, V. L. *J. Am. Chem. Soc.* **1993**, *115*, 5857–5858.
- (16) Bard, A. J.; Abruña, H. A.; Chidsey, C. E.; Faulkner, L. R.; Feldberg, S. W.; Itaya, K.; Majda, M.; Melroy, M.; Murray, R. W.; Porter, M. D.; Soriaga, M. P.; White, H. S. *J. Phys. Chem.* **1993**, *97*, 7147.
- (17) Espinet, P.; Esteruelas, M. A.; Oro, L. A.; Serrano, J. L.; Sola, E. *Coord. Chem. Rev.* **1992**, *117*, 215.
- (18) Giroud-Godquin, A. M.; Maitlis, P. M. *Angew. Chem., Int. Ed. Engl.* **1991**, *30*, 375.
- (19) Hudson, S. A.; Maitlis, P. M. *Chem. Rev.* **1993**, *93*, 861.

- (20) The nomenclature for metallacrowns is: $M'_m A_a [X-MC_{M^+H(Z)-Y}]$ where X and Y indicate ring size and number of oxygen donor atoms, MC specifies a metallacrown, M and $n+$ are the ring metal and its oxidation state, H is the identity of the remaining heteroatom bridge and (Z) is an abbreviation for the organic ligand containing the hydroximate functionality. There are m' captured metals (M') and a bridging anions (A) bound to the ring oxygens and metals, respectively. A metal encapsulated metallacrown is represented by [Cu^{II}(12-MC_{Cu(II)N(anha)⁻⁴)]²⁻, **1a**. This molecule has the core structure of 12-crown-4 with the carbon atoms replaced by Cu(II) and N atoms throughout the ring. The doubly deprotonated form of anthranilic hydroxamic acid (anha²⁻) confers stability to the ring. A Cu(II) resides in the core bound by the four hydroximate oxygens.}
- (21) These supporting organic ligands have either two or three protonation states and several ligation modes. The hydroxamic acid is the fully protonated uncoordinated ligand. A single deprotonation yields the hydroxamate that can ligate to a metal via the hydroxamate carbonyl oxygen and oxime oxygen in a five membered chelate. Double deprotonation of hydroxamic acid moiety affords the hydroximate which forms an analogous five-membered chelate. Fully deprotonated, shi³⁻ has several distinct modes of metal coordination, two of which are observed in metallacrown structures. First, a hydroximate chelate can be formed by the hydroximate oxygens. Second, the six-membered iminophenolate chelate can be formed from the phenolate oxygen and hydroximate nitrogen. In cases where the metallacrown encapsulates a metal, the oxime oxygen of the hydroximate bridges from the ring metal to the core metal. For a thorough discussion of hydroxamic acid deprotonation see: Ventura, O. N.; Rama, J. B.; Turi, L.; Dannenberg, J. J. *J. Am. Chem. Soc.* **1993**, *113*, 5754.

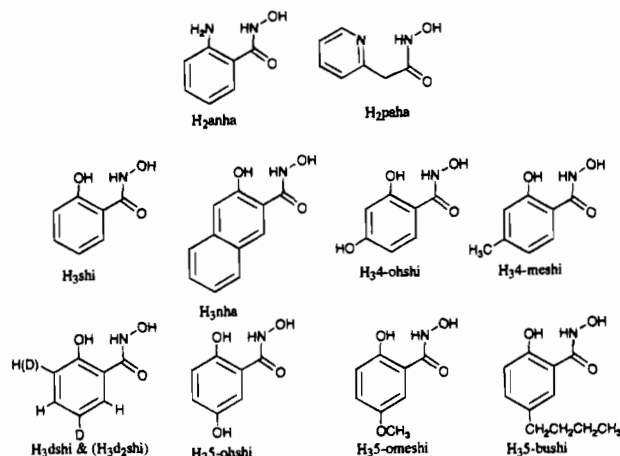


Figure 2. Ligands used in this study. Abbreviations key is given in the text.

2-pyridylacetic acid hydrochloride, 3-hydroxy-2-naphthoic acid, 3,5-diiodosalicylic acid, 5-iodosalicylic acid, 2,4-dihydroxybenzoic acid, 2,5-dihydroxybenzoic acid, 4-methylsalicylic acid, 5-methoxysalicylic acid, salicylic acid, butyryl chloride, and hydroxylamine hydrochloride were obtained from Aldrich Chemical Co. All other chemicals and solvents were reagent grade.

Abbreviations Used. H₂anha = anthranilic hydroxamic acid; H₂paha = 2-pyridylaceto hydroxamic acid; H₃nha = 3-hydroxy-2-naphtho hydroxamic acid; H₃shi = salicylhydroxamic acid; H₃dshi = 5-deuteriosalicylhydroxamic acid; H₃d₂shi = 3,5-dideuteriosalicylhydroxamic acid; H₃4-ohshi = 2,4-dihydroxybenzohydroxamic acid; H₃4-meshi = 4-methylsalicylhydroxamic acid; H₃5-ohshi = 2,5-dihydroxybenzohydroxamic acid; H₃5-omeshi = 5-methoxysalicylhydroxamic acid, H₃5-bushi = 5-butylsalicylhydroxamic acid, 15-C-5 = 1,4,7,10,13-pentaoxacyclopentadecane (Figure 2).

Preparations of Ligands and Complexes. Anthranilic Hydroxamic Acid. Ethyl-2-amino benzoate (16.5 g, 100 mmol) was condensed with hydroxylamine hydrochloride (13.9 g, 200 mmol) and KOH (16.8 g, 300 mmol) in methanol. After 2 days, the salt of the hydroxamic acid crystallized and was filtered. The filtrate was washed with ether and redissolved in a methanol solution of CH₃COOH (1.25 M). The resulting anthranilic hydroxamic acid, H₂anha, crystallized from the solution (8.7 g, 57% yield based on ester). Anal. Calcd for C₇H₈N₂O₂: C, 55.2; H, 5.3; N, 18.4. Found: C, 55.1; H, 5.4; N, 18.5. ¹H NMR in MeOD-*d*₄: δ 6.59 (t, 1H), 6.74 (d, 1H), 7.17 (t of d, 1H), 7.29 (d of d, 1H). HRMS: predicted *m/z* 152.0586, observed *m/z* 152.0590.

Additional Ligands. The ligands 2-pyridylaceto hydroxamic acid, 4-methylsalicylhydroxamic acid, 5-hydroxysalicylhydroxamic acid, 5-methoxysalicylhydroxamic acid, and 5-butylsalicylhydroxamic acid were prepared in an analogous manner to that used for anthranilic hydroxamic acid. The ligands 3-hydroxy-2-naphtho hydroxamic acid, 3-deuteriosalicylhydroxamic acid, 3,5-dideuteriosalicylhydroxamic acid, and 2,4-dihydroxybenzohydroxamic acid were prepared as previously described.⁹ All ligands gave satisfactory ¹³C NMR and HRMS data.

Complexes of H₂L. [Cu^{II}(12-MC_{Cu(II)N(anha)}-4)]Cl₂·2H₂O, **1a**. CuCl₂·xH₂O (1.28 g, 6.25 mmol) and sodium acetate (0.84 g, 10 mmol) were dissolved in 75 mL of MeOH. A 60 mL solution of MeOH containing H₂anha (0.80 g, 5 mmol) was added and allowed to stir for 1.5 h during which time the product precipitated yielding 0.943 g (74%) of green powder. Anal. Calcd for Cu₅C₂₈H₂₈N₈O₁₀Cl₂: Cu, 30.1; C, 32.8; H, 2.7; N, 10.9. Found: Cu, 31.0; C, 32.7; H, 2.8; N, 10.5. ESI-MS(+) molecular ion at *m/z* 918 (42% of base); intact ion at *m/z* 459 (base).

[Cu^{II}(12-MC_{Cu(II)N(anha)}-4)](ClO₄)₂·3MeOH, **1b**. *Caution: Perchlorate salts are potentially explosive. They should only be synthesized in small quantities and should be treated with utmost care at all times.* Cu(ClO₄)₂ (0.23 g, 0.63 mmol) and sodium acetate (0.08 g, 1 mmol) were dissolved in 5 mL of MeOH. A 5 mL solution of MeOH containing H₂anha (0.08 g, 0.5 mmol) was added and allowed to stir for 1.5 h before gravity filtration. Slow evaporation of the filtrate yielded 0.118 g (85%) of green crystals. Anal. Calcd for

Cu₅C₂₈H₂₄N₈O₁₆Cl₂: Cu, 28.4; C, 30.0; H, 2.1; N, 10.0. Found: Cu, 28.4; C, 29.6; H, 2.3; N, 9.6. ESI-MS(+) molecular ion at *m/z* 918 (20% of base); intact ion at *m/z* 459 (base).

[Cu^{II}(12-MC_{Cu(II)N(paha)}-4)]Cl₂, **2**. CuCl₂·xH₂O (1.28 g, 6.25 mmol) was dissolved in 50 mL of MeOH. A 60 mL solution of MeOH containing H₂paha (0.78 g, 5 mmol) and sodium acetate (0.84 g, 10 mmol) was added and allowed to stir for 3 h during which time the metallacrown precipitated, yielding 1.05 g (85%) of green powder. Anal. Calcd for Cu₅C₂₈H₂₄N₈O₈Cl₂: Cu, 32.1; C, 34.0; H, 2.4; N, 11.3. Found: Cu, 31.9; C, 33.6; H, 2.6; N, 11.0. ESI-MS(+) molecular ion at *m/z* 918 (22% of base); intact ion at *m/z* 459 (base).

Complexes of H₃L. (TEA)₂[Cu^{II}(12-MC_{Cu(II)N(nha)}-4)]·DMF, **3**. Cu(OAc)₂ (1.25 g, 6.25 mmol) and tetraethylammonium acetate (2.60 g, 10 mmol) were dissolved in 50 mL of DMF. A 50 mL solution of DMF containing H₃nha (1.01 g, 5 mmol) was added and allowed to stir for 2 h before gravity filtration. Vapor diffusion of diethyl ether afforded 1.320 g (77%) of forest green crystalline rods. Anal. Calcd for Cu₅C₆₀H₆₄N₆O₁₂: Cu, 23.0; C, 52.2; H, 4.7; N, 6.1. Found: Cu, 22.4; C, 51.6; H, 5.1; N, 6.1. FAB-MS(-) molecular ion at *m/z* 1118 (88% of base).

(Na(15-C-5))₂[Cu^{II}(12-MC_{Cu(II)N(shi)}-4)]·MeOH, **4a**. Cu(OAc)₂ (1.25 g, 6.25 mmol) and sodium acetate (0.83 g, 10 mmol) were dissolved in 50 mL of MeOH. A 50 mL solution of MeOH containing H₃shi (0.77 g, 5 mmol) was added and allowed to stir for 15 min as a green precipitate formed in >90% yield. The precipitate was filtered, washed with MeOH, and dried. The dried powder was dissolved in MeOH by addition of 1 equiv of 15-C-5 (0.55 g, 2.5 mmol) per sodium. An X-ray quality crystal of **4a** was obtained by cooling a dilute solution of **4a** in MeOH to -20 °C and adding a drop of MeOH concentrated with **4a** daily. Anal. Calcd for Cu₅Na₂C₃₉H₆₀N₄O₂₃: Cu, 22.1; Na, 3.9; C, 40.1; H, 4.2; N, 3.9. Found: Cu, 22.7; Na, 3.6; C, 39.6; H, 4.2; N, 3.8. FAB-MS(-) molecular ion at *m/z* 918 (90% of base).

(TMA)₂[Cu^{II}(12-MC_{Cu(II)N(shi)}-4)]·DMF, **4b**. Cu(OAc)₂ (1.25 g, 6.25 mmol), tetramethylammonium acetate (1.30 g, 10 mmol), and H₃shi (0.77 g, 5 mmol) were dissolved in 125 mL of DMF. The solution allowed to stir for 4 h before gravity filtration. Vapor diffusion of diethyl ether afforded 0.983 g (74%) of crystalline rods of **4b**. Anal. Calcd for Cu₅C₃₉H₄₇N₅O₁₃: Cu, 28.6; C, 41.1; H, 4.2; N, 8.6. Found: Cu, 28.1; C, 41.3; H, 4.2; N, 9.0.

(TMA)₂[Cu^{II}(12-MC_{Cu(II)N(dshi)}-4)]·4H₂O, **5a**. A 50 mL solution containing 5-deuteriosalicylhydroxamic acid (H₃dshi) (0.78 g, 5 mmol) and tetramethylammonium acetate (1.30 g, 10 mmol) was added to a solution of Cu(OAc)₂ (1.25 g, 6.25 mmol) in 100 mL of MeOH. The resulting solution was allowed to stir 10 min before gravity filtration. The product crystallized overnight to yield 1.37 g (96%) of the metallacrown. Anal. Calcd for Cu₅C₃₆H₄₈D₄N₆O₁₆: Cu, 27.7; C, 37.7; H, 4.9; N, 7.3. Found: Cu, 27.3; C, 37.5; H, 4.7; N, 7.2. ESI-MS(-) **5a** molecular ion at *m/z* 922 (base).

(TEA)₂[Cu^{II}(12-MC_{Cu(II)N(dzshi)}-4)]·2DMF·H₂O, **5b**. Cu(OAc)₂ (1.25 g, 6.25 mmol), tetraethylammonium acetate (1.90 g, 10 mmol) and H₃d₂shi (0.78 g, 5 mmol) were dissolved in 125 mL of DMF. The solution allowed to stir for 12 h before gravity filtration. Vapor diffusion of diethyl ether afforded 0.845 g (50%) of crystalline rods of **5b**. Anal. Calcd for Cu₅C₅₀H₆₄D₈N₈O₁₅: Cu, 23.5; C, 44.4; H, 5.9; N, 8.3. Found: Cu, 23.8; C, 44.2; H, 5.7; N, 8.2. ESI-MS(-) molecular ion at *m/z* 926 (base).

(TMA)₂[Cu^{II}(12-MC_{Cu(II)N(4-ohshi)}-4)], **6**. Cu(OAc)₂ (1.25 g, 6.25 mmol) and tetramethylammonium acetate (1.30 g, 10 mmol) were dissolved in 50 mL of DMF. A 50 mL solution of DMF containing H₃4-ohshi (0.83 g, 5 mmol) was added and the resulting solution allowed to stir for 2 h before gravity filtration. The filtrate afforded 1.12 g (79% yield) of crystalline rods upon vapor diffusion of diethyl ether. Anal. Calcd for Cu₅C₃₆H₄₀N₆O₁₆: C, 38.2; H, 3.6; N, 7.4. Found: C, 37.8; H, 3.5; N, 7.8. FAB-MS(-) molecular ion at *m/z* 983 (3.9% of base).

Na₂[Cu^{II}(12-MC_{Cu(II)N(4-meshi)}-4)]·4H₂O, **7**. Cu(OAc)₂ (1.25 g, 6.25 mmol) and sodium acetate (0.84 g, 10 mmol) were dissolved in 50 mL of MeOH. A 50 mL solution of MeOH containing H₃4-meshi (0.85 g, 5 mmol) was added and the solution allowed to stir for 1 h before gravity filtration. The product precipitated as a powder within 5 min of mixing. Gravity filtration of the solution gave 0.973 g (93% yield) of product as green powder. The powder was recrystallized from DMF:

Table 1. Crystal, Data Collection, and Refinement Parameters for $[\text{Cu}^{\text{II}}(12\text{-MC}_{\text{Cu}(\text{II})\text{N}(\text{anha})\text{-4})}](\text{ClO}_4)_2$, **1b**, $(\text{TEA})_2[\text{Cu}^{\text{II}}(12\text{-MC}_{\text{Cu}(\text{II})\text{N}(\text{nha})\text{-4})}]$, **3**, $(\text{Na}(15\text{-C-5}))_2[\text{Cu}^{\text{II}}(12\text{-MC}_{\text{Cu}(\text{II})\text{N}(\text{shi})\text{-4})}]$, **4a**, and $(\text{TMA})_2[\text{Cu}^{\text{II}}(12\text{-MC}_{\text{Cu}(\text{II})\text{N}(\text{shi})\text{-4})}]$, **4b**

	1b	3	4a	4b
formula	$\text{C}_{31.75}\text{H}_{40}\text{N}_8\text{O}_{20.25}\text{Cl}_2\text{Cu}_5$	$\text{C}_{63}\text{H}_{71}\text{N}_7\text{O}_{13}\text{Cu}_5$	$\text{C}_{52.5}\text{H}_{78}\text{N}_4\text{O}_{26.5}\text{Na}_2\text{Cu}_5$	$\text{C}_{42}\text{H}_{54}\text{N}_8\text{O}_{14}\text{Cu}_5$
mol wt	1245	1452.1	1553	1212.6
cryst syst	triclinic	monoclinic	monoclinic	rhombohedral
space group	$P\bar{1}$ (No. 2)	$C2/c$ (No. 15)	$C2/c$ (No. 15)	$R\bar{3}$ (No. 148)
unit cell dimens				
<i>a</i> , Å	11.077(2)	31.600(4)	34.97(1)	33.634(8)
<i>b</i> , Å	12.294(2)	8.108(2)	14.350(6)	33.634(8)
<i>c</i> , Å	17.272(4)	27.180(4)	29.00(2)	11.276(2)
α , deg	110.29(2)	90.000	90.000	90.000
β , deg	96.05(2)	102.97(1)	120.30(4)	120.000
γ , deg	96.27(1)	90.000	90.000	90.000
vol, Å ³	2166.9(7)	6786(2)	12563(10)	11059(5)
Z	2	4	8	9
temp, K	183	178	188	298
radiation (λ)	Mo K α (0.710 73 Å)	Mo K α (0.710 73 Å)	Mo K α (0.710 73 Å)	Mo K α (0.710 73 Å)
quantity minimized	$\sum w(F_o - F_c)^2$	$\sum w(F_o - F_c)^2$	$\sum w(F_o - F_c)^2$	$\sum w(F_o ^2 - F_c ^2)^2$
R	0.0590 ^a	0.0609 ^a	0.1226 ^c	0.1242 ^c
R _w	0.0821 ^b	0.0924 ^b	0.0840 ^b	N/A

^a $R = \sum ||F_o| - |F_c|| / \sum |F_o|$. ^b $R_w = [\sum w(|F_o| - |F_c|)^2 / \sum w|F_o|]^2$. ^c $wR^2 = [\sum w(F_o^2 - F_c^2)^2 / \sum w(F_o^2)^2]^{1/2}$. For comparison with structures refined on F_o , the conventional residual for $F_o \geq 4\sigma F_o$ is 0.0423.

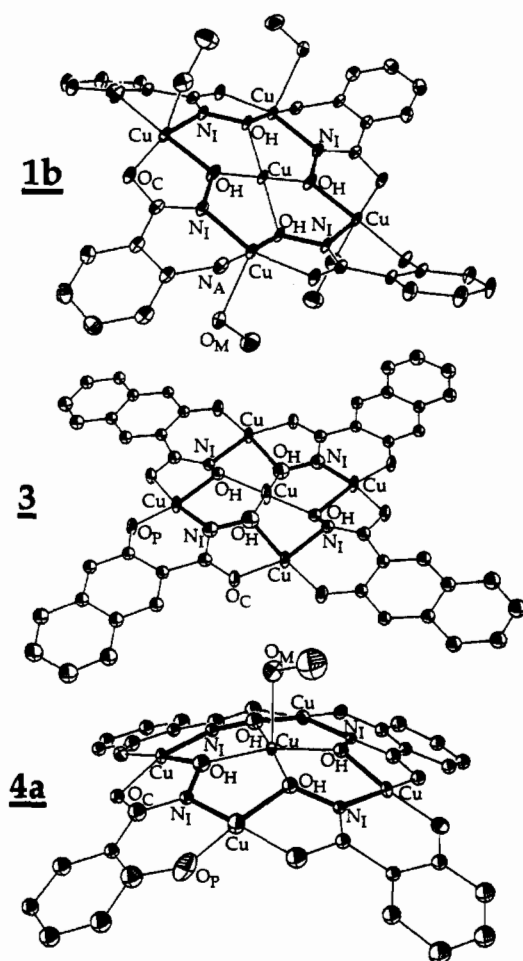


Figure 3. ORTEP diagrams of $[\text{Cu}^{\text{II}}(12\text{-MC}_{\text{Cu}(\text{II})\text{N}(\text{anha})\text{-4})}]^{2+}$, **1b**, with thermal ellipsoids at 50% probability; $[\text{Cu}^{\text{II}}(12\text{-MC}_{\text{Cu}(\text{II})\text{N}(\text{nha})\text{-4})}]^{2+}$, **3**, with thermal ellipsoids at 50% probability; $[\text{Cu}^{\text{II}}(12\text{-MC}_{\text{Cu}(\text{II})\text{N}(\text{shi})\text{-4})}]^{2+}$, **4a**, with thermal ellipsoids at 20% probability. The metallacrown ring, $[\text{Cu}(\text{II})\text{-N}_1\text{-O}_H]_4$, is in boldface. The heteroatoms of one of the four metallacrown ligands are labeled (O_p = phenolate oxygen; O_H = hydroximate oxygen; O_c = carbonyl oxygen; N_A = amine nitrogen; N_I = imine nitrogen; O_M = methanol oxygen) in each ORTEP diagram. The numbering scheme has been simplified and the hydrogen atoms are omitted for clarity.

H_2O (20:1) via vapor diffusion of ether. Anal. Calcd for $\text{Cu}_5\text{Na}_2\text{C}_{32}\text{H}_{32}\text{N}_4\text{O}_{16}$: Cu, 29.0; Na, 4.2; C, 35.2; H, 2.9; N, 5.1.

Found: Cu, 27.6; Na, 4.7; C, 35.6; H, 3.0; N, 4.7. ESI-MS(-) molecular ion at m/z 975 (base).

$(\text{TMA})_2[\text{Cu}^{\text{II}}(12\text{-MC}_{\text{Cu}(\text{II})\text{N}(\text{s-ohshi})\text{-4})}]$, **8**. $\text{Cu}(\text{OAc})_2$ (1.25 g, 6.25 mmol) and tetramethylammonium acetate (1.30 g, 10 mmol) were dissolved in 50 mL of DMF. A 50 mL DMF solution containing $\text{H}_3\text{S-ohshi}$ (0.83 g, 5 mmol) was added and allowed to stir for 1.5 h before gravity filtration. Vapor diffusion of diethyl ether afforded 1.03 g (69% yield) of crystalline rods. Anal. Calcd for $\text{Cu}_5\text{C}_{36}\text{H}_{40}\text{N}_6\text{O}_{16}$: Cu, 28.1; C, 38.3; H, 3.6; N, 7.4. Found: Cu, 29.0; C, 37.9; H, 4.0; N, 7.6. ESI-MS(-) molecular ion at m/z 983 (base).

$\text{K}^+_2[\text{Cu}^{\text{II}}(12\text{-MC}_{\text{Cu}(\text{II})\text{N}(\text{s-omeshi})\text{-4})}]4\text{DMF}$, **9**. $\text{Cu}(\text{OAc})_2$ (1.25 g, 6.25 mmol) and potassium acetate (0.98 g, 10 mmol) were dissolved in 50 mL of DMF. A 50 mL solution of DMF containing $\text{H}_3\text{S-omeshi}$ (0.86 g, 5 mmol) was added and the solution allowed to stir for 1 h before gravity filtration. The product precipitated affording 0.964 g (86% yield) of olive green powder. Anal. Calcd for $\text{Cu}_5\text{K}_2\text{C}_{44}\text{H}_{52}\text{N}_6\text{O}_{20}$: K, 5.5; C, 37.5; H, 3.7; N, 7.9. Found: K, 5.5; C, 37.4; H, 3.8; N, 7.8. ESI-MS(-) molecular ion at m/z 1037 (base).

$\text{K}^+_2[\text{Cu}^{\text{II}}(12\text{-MC}_{\text{Cu}(\text{II})\text{N}(\text{s-bushi})\text{-4})}]$, **10**. $\text{Cu}(\text{OAc})_2$ (1.25 g, 6.25 mmol) and potassium acetate (0.98 g, 10 mmol) were dissolved in 150 mL of MeOH. A 100 mL solution of MeOH containing $\text{H}_3\text{S-bushi}$ (1.05 g, 5 mmol) was added and the solution allowed to stir for 1 h before gravity filtration. The product precipitated as a green powder overnight affording 0.771 g (63% yield) of olive green powder. Anal. Calcd for $\text{Cu}_5\text{K}_2\text{C}_{44}\text{H}_{52}\text{N}_4\text{O}_{12}$: Cu, 25.9; K, 6.3; C, 43.1; H, 4.2; N, 4.6. Found: Cu, 25.5; K, 6.0; C, 42.7; H, 4.3; N, 4.6. ESI-MS(-) molecular ion $[\text{M}^-]$ at m/z 1143 (10% of base), intact ion $[\text{M}^{2-}]$ at m/z 572 (34% of base), $[\text{M}^{2-} + \text{K}^+]^-$ at m/z 1181 (base).

$9\text{-MC}_{(\text{V}(\text{VO})\text{N}(\text{nha})\text{-3})}$, **11**. The vanadium metallacrown was prepared by the literature procedure.⁹

Characterization Methods. ¹H NMR and ¹³C spectra were obtained on a Bruker 360 MHz FT-NMR spectrometer operating in the quadrature detection mode (¹H frequency, 360.1 MHz). Chemical shifts were referenced to TMS or resonances due to residual protons present in the deuterated solvents. UV-visible spectra were recorded on a Perkin-Elmer Lambda 9 UV/vis/near-IR spectrophotometer equipped with a Perkin-Elmer 3600 data station. Variable temperature magnetic susceptibility data was collected with a Quantum Concepts SQUID magnetometer. Molecular modeling was performed using Biosym Technologies Insight II on a Silicon Graphics Indigo workstation. Positive and negative FAB mass spectra were acquired by the University of Michigan Mass Spectroscopy Facility. Positive and negative electrospray ionization mass spectra were acquired by the University of Michigan Protein and Carbohydrate Structure Facility. Elemental analyses were performed by the Microanalysis Laboratory in the Department of Chemistry at the University of Michigan.

Collection and Reduction of X-ray Data. Suitable crystals of **1b**, **3**, **4a**, and **4b** were obtained as described above. These crystals were

Table 2. Fractional Atomic Coordinates for $[\text{Cu}^{\text{II}}(12\text{-MC}_{\text{Cu}(\text{II})\text{N}(\text{anha})\text{-4})](\text{ClO}_4)_2$, **1b**

atom	x	y	z	$U_{\text{eq}},^a \text{ \AA}^2$	atom	x	y	z	$U_{\text{eq}},^a \text{ \AA}^2$
Cu(1)	0.41219(4)	0.58845(4)	0.68490(3)	0.0138(2)	N(2)	0.3819(3)	0.4214(3)	0.6149(2)	0.015(1)
Cu(1a)	0.58781(4)	0.41155(4)	0.31509(3)	0.0138(2)	N(3)	0.4175(3)	0.0620(3)	0.4138(2)	0.016(1)
Cu(2)	0.39572(4)	0.22801(4)	0.47160(3)	0.0138(2)	N(4)	0.4634(3)	0.2646(3)	0.3828(2)	0.016(1)
Cu(3)	0.50000	0.50000	0.50000	0.0133(2)	N(5)	0.2787(3)	0.3932(3)	0.1263(2)	0.019(1)
Cu(4)	0.16386(4)	0.25549(4)	0.04769(3)	0.0133(2)	N(6)	0.1503(3)	0.1903(3)	0.1354(2)	0.015(1)
Cu(4a)	-0.16386(4)	-0.25549(4)	-0.04769(3)	0.0133(2)	N(7)	-0.0067(4)	-0.0278(3)	0.2867(2)	0.021(1)
Cu(5)	0.03559(4)	0.03034(4)	0.19704(3)	0.0152(2)	N(8)	-0.0573(3)	-0.1133(3)	0.1140(2)	0.015(1)
Cu(6)	0.00000	0.00000	0.00000	0.0136(2)	C(1)	0.3770(3)	0.4452(3)	0.7904(2)	0.015(1)
Cl(1)	0.86436(9)	0.28570(8)	0.08909(6)	0.0204(3)	C(2)	0.4006(4)	0.4507(4)	0.8728(3)	0.020(1)
Cl(2)	0.75418(8)	0.10741(8)	0.44318(6)	0.0180(3)	C(3)	0.4284(4)	0.3538(4)	0.8910(3)	0.023(1)
O(1)	0.3772(3)	0.2239(2)	0.5804(2)	0.0173(9)	C(4)	0.4309(4)	0.2487(4)	0.8250(3)	0.024(1)
O(2)	0.3873(2)	0.3934(2)	0.5284(2)	0.0155(9)	C(5)	0.4080(4)	0.2424(4)	0.7430(3)	0.020(1)
O(2a)	0.6127(2)	0.6065(2)	0.4716(2)	0.0155(9)	C(6)	0.3837(3)	0.3401(3)	0.7239(2)	0.014(1)
O(3)	0.5124(3)	0.2444(2)	0.2539(2)	0.0174(9)	C(7)	0.3779(3)	0.3268(3)	0.6345(2)	0.014(1)
O(3a)	0.4876(3)	0.7556(2)	0.7461(2)	0.0174(9)	C(8)	0.3740(3)	0.0122(3)	0.3242(2)	0.015(1)
O(4)	0.5253(3)	0.3782(2)	0.4038(2)	0.021(1)	C(9)	0.3083(4)	-0.1005(3)	0.2894(3)	0.020(1)
O(4a)	0.4747(3)	0.6218(2)	0.5962(2)	0.021(1)	C(10)	0.2665(4)	-0.1529(4)	0.2049(3)	0.024(1)
O(5)	0.1302(3)	0.1858(2)	0.2643(2)	0.0177(9)	C(11)	0.2928(4)	-0.0908(4)	0.1523(3)	0.024(1)
O(6)	0.0948(3)	0.0738(2)	0.1098(2)	0.0175(9)	C(12)	0.3583(4)	0.0218(4)	0.1866(3)	0.020(1)
O(6a)	-0.0948(3)	-0.0738(2)	-0.1098(2)	0.0175(9)	C(13)	0.3996(3)	0.0760(3)	0.2720(2)	0.015(1)
O(7)	-0.1558(3)	-0.3013(2)	0.0500(2)	0.0183(9)	C(14)	0.4625(3)	0.2002(3)	0.3037(2)	0.015(1)
O(7a)	0.1558(3)	0.3013(2)	-0.0500(2)	0.0183(9)	C(15)	0.2712(3)	0.4389(3)	0.2152(2)	0.016(1)
O(8)	-0.0967(3)	-0.1063(2)	0.0355(2)	0.0162(9)	C(16)	0.3135(4)	0.5582(4)	0.2599(3)	0.021(1)
O(8a)	0.0967(3)	0.1063(2)	-0.0355(2)	0.0162(9)	C(17)	0.3139(4)	0.6085(4)	0.3450(3)	0.024(1)
O(9)	0.2229(3)	0.6465(3)	0.6523(2)	0.026(1)	C(18)	0.2699(4)	0.5387(4)	0.3876(3)	0.022(1)
O(10)	0.1887(3)	0.1692(3)	0.4151(2)	0.0196(9)	C(19)	0.2263(4)	0.4207(4)	0.3444(2)	0.019(1)
O(11)	-0.1511(3)	0.1149(3)	0.2254(2)	0.026(1)	C(20)	0.2240(3)	0.3682(3)	0.2579(2)	0.015(1)
O(12)	0.5224(3)	0.7456(3)	0.9001(2)	0.026(1)	C(21)	0.1671(3)	0.3623(3)	0.2171(2)	0.015(1)
O(13)	0.8709(3)	0.3169(3)	0.1784(2)	0.029(1)	C(22)	-0.0164(3)	-0.1531(3)	0.2724(2)	0.016(1)
O(14)	0.7562(3)	0.3226(3)	0.0577(2)	0.032(1)	C(23)	0.0222(4)	-0.1831(4)	0.3405(2)	0.019(1)
O(15)	0.8561(3)	0.1610(3)	0.0490(2)	0.030(1)	C(24)	0.0185(4)	-0.3006(4)	0.3310(3)	0.024(1)
O(16)	0.9715(3)	0.3446(3)	0.0719(2)	0.035(1)	C(25)	-0.0233(4)	-0.3878(4)	0.2533(3)	0.027(2)
O(17)	0.6812(3)	0.1064(3)	0.5080(2)	0.029(1)	C(26)	-0.0631(4)	-0.3566(4)	0.1859(3)	0.024(1)
O(18)	0.6739(3)	0.0600(3)	0.3641(2)	0.037(1)	C(27)	-0.0597(3)	-0.2396(3)	0.1939(2)	0.017(1)
O(19)	0.8493(3)	0.0388(3)	0.4434(2)	0.037(1)	C(28)	-0.0943(3)	-0.2167(3)	0.1156(2)	0.016(1)
O(20)	0.8066(3)	0.2269(3)	0.4587(2)	0.033(1)	C(29)	0.1115(5)	0.5742(5)	0.6114(4)	0.042(2)
O(21)	0.213(1)	0.5512(9)	0.0487(6)	0.050(2)	C(30)	0.1131(4)	0.2275(4)	0.4750(3)	0.033(2)
O(22)	-0.156(1)	-0.5629(9)	-0.0673(6)	0.056(2)	C(31)	-0.2675(4)	0.0529(4)	0.1810(3)	0.032(2)
N(1)	0.3461(3)	0.5480(3)	0.7755(2)	0.018(1)	C(32)	0.5200(7)	0.8426(5)	0.9734(3)	0.043(2)
C(33)	-0.260(2)	-0.570(2)	-0.061(1)	0.069(5)					

$$^a U_{\text{eq}} = (1/3) \sum_i \sum_j U_{ij} a_i^* a_j^* a_i a_j$$

mounted in glass capillaries. Principle experimental parameters are given in Table 1. The data were reduced, the structure was solved via direct methods and the model was refined using either the SHELXTL PLUS^{22a} program package (for **1b**, **3**, and **4a**) or the SHELEX-93^{22b} program package (**4b**) on a VAX Station 3500. Catastrophic crystal damage of **4a** prevented collection of $2\theta > 40^\circ$ data. Due to the observed disorder in the organic crowns in **4a** a crystal of **4** suitable for X-ray analysis was grown with tetramethylammonium cations, **4b**. The ORTEP of **4a** is presented in Figure 3 to establish the connectivity and conformation of the complex. Fractional atomic coordinates for **1b**, **3**, and **4b** are given in Tables 2–4, respectively. Selected average interatomic bond distances for **1b**, **3**, **4a**, and **4b** are given in Table 5. Selected interatomic bond angles for **1b**, **3**, **4a**, and **4b** are presented in Table 6. Fractional atomic coordinates for **4a** are provided in supplementary material.

Results

General Description of $[\text{Cu}^{\text{II}}(12\text{-MC}_{\text{Cu}(\text{II})\text{N}-4)]$ Structures.

The Cu(II) metallacrowns formed from anthranilic hydroxamic acid, **1b**, 3-hydroxy-2-naphthohydroxamic acid, **3**, and salicylhydroxamic acid, **4a**, are illustrated in Figure 3. Chemically equivalent bond distances for the compounds are given in Table 5. Selected interatomic bond angles are provided in Table 6. We will provide a few general comments regarding the basic 12-metallacrown-4 structure of these materials before commenting specifically about the subtleties of each structure.

The complexes are of the 12-MC-4 structural motif with four ring Cu(II) ions and one additional encapsulated Cu(II) ion. The architecture of the metallacrown rings are constructed from four ligands (anha²⁻, nha³⁻, or shi³⁻) linked via four copper(II) ions. The deprotonated hydroxamic acids act as binucleating ligands with the carbonyl and hydroxamate oxygens (O_C and O_H) bound to one copper(II) and the aryl amine nitrogen (N_A) or phenolate oxygen (O_P) plus imine nitrogens (N_I) chelating an adjacent copper(II). The juxtaposed five-membered and six-membered chelates form the basis of metallacrown structures through a $[\text{Cu}(\text{II})\text{-N}_I\text{-O}_H\text{-}]_4$ ring system that is analogous to a 12-C-4 with the methylene carbons replaced with Cu(II) and N. The average nearest neighbor ring copper ion separation is 4.59 Å. The average cavity size is 0.65 Å, which allows encapsulation of a fifth cupric ion (Cu(II), four coordinate ionic radius = 0.57 Å)²³ in the metallacrown core. The central copper(II) can be either square planar, square pyramidal, or octahedral with the square planar geometry placing the copper in the best least squares plane of the four metallacrown oxygens. The ring Cu(II) to central Cu(II) average distance is 3.27 Å, a value that is considerably shorter than the ring metal–core metal average separation of 3.47 Å of previous 12-MC-4's based on Mn(III) and Fe(III).^{10,11}

These structures are similar to the previously reported $\{\text{Fe}(\text{SO}_4)_2[12\text{-MC}_{\text{Fe}(\text{III})\text{N}(\text{shi})-4}]\}^-$ metallacrown, but lack bridging anions.¹ Furthermore, the ring metals do not have octahedral

(22) (a) Siemens Analytical Services, Madison, WI, 1988. (b) Sheldrick, G. M. *J. Appl. Crystallogr.*, in press.

(23) Shannon, R. D. *Acta Crystallogr.* **1976**, A32, 751

Table 3. Fractional Atomic Coordinates for (TEA)₂[Cu(12-MC_{Cu(II)N(aha)}-4)], **3**

atom	x	y	z	U _{eq} ^a Å ²
Cu(1)	0.00265(1)	0.01745(7)	-0.11839(2)	0.0260(2)
Cu(2)	-0.09684(1)	0.15863(6)	-0.02580(2)	0.0236(2)
Cu(3)	0.00000	0.00000	0.00000	0.0365(3)
O(1)	-0.02060(8)	0.0666(4)	-0.18571(9)	0.0239(8)
O(2)	-0.11593(8)	0.1901(3)	-0.09981(9)	0.0235(8)
O(3)	-0.0554(1)	0.0131(6)	-0.0500(2)	0.0166(9)
O(3')	0.0490(2)	-0.0809(9)	0.0466(2)	0.019(1)
O(4)	-0.14608(8)	0.2454(4)	-0.00629(9)	0.0265(9)
O(5)	0.06046(8)	-0.0476(3)	-0.12645(9)	0.0237(8)
O(6)	-0.0278(2)	0.044(1)	0.0516(3)	0.030(1)
O(6')	-0.0357(3)	-0.038(1)	0.0495(3)	0.058(2)
N(1)	-0.0486(3)	0.095(1)	-0.0976(3)	0.016(2)
N(1')	-0.0525(2)	0.0450(8)	-0.0996(2)	0.017(1)
N(2)	-0.0746(2)	0.0597(9)	0.0413(2)	0.017(1)
N(2')	-0.0684(2)	0.1264(9)	0.0430(2)	0.014(1)
N(3)	0.50000	0.1097(6)	-0.25000	0.034(2)
N(4)	0.1594(1)	0.3095(5)	0.0810(2)	0.045(2)
C(1)	-0.0598(1)	0.1267(4)	-0.2058(1)	0.020(1)
C(2)	-0.0703(1)	0.1525(4)	-0.2579(1)	0.021(1)
C(3)	-0.1092(1)	0.2245(4)	-0.2829(1)	0.019(1)
C(4)	-0.1187(1)	0.2616(5)	-0.3364(1)	0.029(1)
C(5)	-0.1561(1)	0.3431(5)	-0.3584(2)	0.035(1)
C(6)	-0.1871(1)	0.3901(6)	-0.3303(2)	0.042(2)
C(7)	-0.1790(1)	0.3550(5)	-0.2795(2)	0.032(1)
C(8)	-0.1401(1)	0.2740(5)	-0.2550(1)	0.021(1)
C(9)	-0.1302(1)	0.2434(5)	-0.2026(1)	0.021(1)
C(10)	-0.0913(1)	0.1710(4)	-0.1775(1)	0.018(1)
C(11)	-0.0860(1)	0.1435(5)	-0.1228(1)	0.021(1)
C(12)	-0.1569(1)	0.2284(5)	0.0374(1)	0.019(1)
C(13)	-0.1975(1)	0.2842(5)	0.0423(1)	0.020(1)
C(14)	-0.2137(1)	0.2649(5)	0.0861(1)	0.020(1)
C(15)	-0.2565(1)	0.3116(5)	0.0893(2)	0.024(1)
C(16)	-0.2708(1)	0.2852(5)	0.1328(2)	0.028(1)
C(17)	-0.2433(1)	0.2136(6)	0.1753(2)	0.033(1)
C(18)	-0.2021(1)	0.1631(5)	0.1737(2)	0.033(1)
C(19)	-0.1864(1)	0.1867(5)	0.1293(1)	0.024(1)
C(20)	-0.1443(1)	0.1363(5)	0.1259(1)	0.023(1)
C(21)	-0.1294(1)	0.1553(4)	0.0818(1)	0.019(1)
C(22)	-0.0850(1)	0.0937(5)	0.0842(1)	0.025(1)
C(23)	0.5073(2)	-0.0024(5)	-0.2044(2)	0.042(2)
C(24)	0.5174(2)	0.0803(7)	-0.1541(2)	0.059(2)
C(25)	0.4611(2)	0.2246(6)	-0.2536(2)	0.044(2)
C(26)	0.4182(2)	0.1419(6)	-0.2560(2)	0.047(2)
C(27)	0.1729(2)	0.1812(6)	0.1189(2)	0.055(2)
C(28)	0.1932(2)	0.233(1)	0.1724(2)	0.077(3)
C(29)	0.1288(2)	0.4306(7)	0.0975(2)	0.059(2)
C(30)	0.0896(2)	0.3548(9)	0.1110(3)	0.079(3)
C(31)	0.1368(2)	0.2262(7)	0.0322(2)	0.058(2)
C(32)	0.1214(2)	0.3410(8)	-0.0129(2)	0.073(3)
C(33)	0.1972(2)	0.4104(7)	0.0732(2)	0.057(2)
C(34)	0.2304(2)	0.3197(9)	0.0521(3)	0.084(3)
O(7)	-0.0515(2)	0.375(1)	-0.0176(3)	0.043(3)
O(8)	0.0162(3)	0.268(1)	0.0001(5)	0.084(5)
N(5)	-0.0095(3)	0.408(1)	-0.0071(4)	0.066(4)

$$^a U_{eq} = (1/3) \sum_i \sum_j U_{ij} a_i^* a_j^* a_i a_j$$

coordination which is most likely a result of the Jahn–Teller elongation in the d⁹ Cu(II) ion. Similar forces drive the d⁴ Mn(III) metallacrowns into the 12-MC-4 motif.^{10,11} While the Mn(OAc)₂[12-MC_{Mn(III)N(shi)}-4] utilizes acetates to bridge to the encapsulated Mn(II), the preference for four-coordinate square planar coordination of the central Cu(II) ion in the [Cu^{II}(12-MC_{Cu(II)N(ligand)}-4)] obviates the need for such bridging anions.¹⁰ The use of a dianionic ligand, anha²⁻, with divalent ring metals results in a formally neutral metallacrown ring that sequesters a Cu(II) to give an overall +2 charge to the complex while a trivalent ligand, shi³⁻, yields an anionic metallacrown with -2 charge.

Description of Structure of [Cu^{II}(12-MC_{Cu(II)N(aha)}-4)](ClO₄)₂, **1b.** *Caution: Perchlorate salts are potentially explo-*

Table 4. Fractional Atomic Coordinates for (TMA)₂[Cu(12-MC_{Cu(II)N(shi)}-4)], **4b**

atom	x	y	z	U _{eq} ^a Å ²
Cu(1)	0.4254(1)	-0.0753(1)	-0.1827(1)	0.043(1)
Cu(2)	0.4849(1)	0.0797(1)	-0.1211(1)	0.042(1)
Cu(3)	0.5000	0.0000	0.0000	0.042(1)
O(1)	0.3858(1)	-0.0927(1)	-0.3115(3)	0.055(1)
O(2)	0.4422(1)	0.0528(1)	-0.2561(3)	0.043(1)
O(3)	0.4636(1)	0.0162(1)	-0.0925(3)	0.049(1)
O(4)	0.4977(1)	0.1410(1)	-0.1346(3)	0.049(1)
O(5)	0.5810(1)	0.1356(1)	0.1498(3)	0.048(1)
O(6)	0.5283(1)	0.0585(1)	0.0663(3)	0.069(1)
N(1)	0.4360(1)	-0.0165(1)	-0.1857(2)	0.045(1)
N(2)	0.5219(1)	0.0937(1)	0.0122(2)	0.051(1)
C(1)	0.3796(1)	-0.0637(2)	-0.3790(4)	0.044(1)
C(2)	0.3514(2)	-0.0844(2)	-0.4801(4)	0.051(2)
C(3)	0.3421(2)	-0.0590(2)	-0.5634(5)	0.055(2)
C(4)	0.3596(2)	-0.0138(2)	-0.5470(6)	0.067(2)
C(5)	0.3862(1)	0.0069(1)	-0.4450(4)	0.041(1)
C(6)	0.3976(1)	-0.0168(2)	-0.3645(4)	0.038(1)
C(7)	0.4271(1)	0.0088(1)	-0.2642(4)	0.041(1)
C(8)	0.5297(1)	0.1768(1)	-0.0759(4)	0.040(1)
C(9)	0.5383(2)	0.2200(2)	-0.1141(5)	0.051(2)
C(10)	0.5706(2)	0.2600(2)	-0.0621(6)	0.063(2)
C(11)	0.5959(2)	0.2598(2)	0.0385(5)	0.058(2)
C(12)	0.5890(1)	0.2165(2)	0.0716(5)	0.047(1)
C(13)	0.5561(1)	0.1754(1)	0.0178(4)	0.038(1)
C(14)	0.5543(2)	0.1332(1)	0.0653(4)	0.042(1)
Cu(1')	0.4384(1)	-0.0995(1)	-0.1290(1)	0.038(1)
Cu(2')	0.4581(1)	0.0455(1)	-0.1790(1)	0.038(1)
O(7)	0.4164(1)	-0.1622(1)	-0.1463(4)	0.051(1)
O(8)	0.4847(1)	0.1114(1)	-0.1404(3)	0.041(1)
O(9)	0.4867(1)	0.0472(1)	-0.0307(3)	0.040(1)
O(10)	0.4267(1)	0.0443(1)	-0.3151(3)	0.042(1)
O(11)	0.4057(1)	-0.0921(1)	-0.2628(3)	0.043(1)
O(12)	0.5496(1)	0.0395(1)	0.0985(3)	0.047(1)
C(15)	0.4260(2)	-0.1881(2)	-0.0706(5)	0.039(2)
C(16)	0.3996(2)	-0.2354(2)	-0.0890(7)	0.050(2)
C(17)	0.4045(2)	-0.2655(2)	-0.0096(7)	0.052(2)
C(18)	0.4358(2)	-0.2512(2)	0.0745(7)	0.054(2)
C(19)	0.4618(2)	-0.2034(2)	0.0903(6)	0.044(2)
C(20)	0.4582(2)	-0.1723(2)	0.0239(6)	0.038(2)
C(21)	0.4870(2)	-0.1227(2)	0.0528(5)	0.035(1)
C(22)	0.4005(2)	0.0073(2)	-0.3850(5)	0.037(1)
C(23)	0.3803(2)	0.0162(2)	-0.4800(6)	0.040(2)
C(24)	0.3525(2)	-0.0174(3)	-0.5535(6)	0.049(2)
C(25)	0.3458(3)	-0.0639(2)	-0.5376(6)	0.054(2)
C(26)	0.3673(2)	-0.0707(2)	-0.4476(6)	0.045(2)
C(27)	0.3938(2)	-0.0365(2)	-0.3664(5)	0.037(2)
C(28)	0.4125(2)	-0.0502(2)	-0.2687(5)	0.038(1)
N(3)	0.5359(1)	0.1468(1)	0.4811(2)	0.055(1)
C(29)	0.5225(1)	0.1575(1)	0.5970(3)	0.094(1)
C(30)	0.5393(1)	0.1792(1)	0.3904(3)	0.113(1)
C(31)	0.5808(1)	0.1494(1)	0.4926(4)	0.093(1)
C(32)	0.5023(2)	0.1008(2)	0.4483(5)	0.146(3)
O(13)	0.8692(1)	0.1244(1)	0.3910(3)	0.139(2)
N(4)	0.7974(1)	0.0892(1)	0.4623(3)	0.067(1)
C(33)	0.7836(2)	0.1166(1)	0.3974(5)	0.120(2)
C(34)	0.7632(1)	0.0518(1)	0.5354(4)	0.092(1)
C(35)	0.8385(1)	0.0931(1)	0.4543(4)	0.101(2)

$$^a U_{eq} = (1/3) \sum_i \sum_j U_{ij} a_i^* a_j^* a_i a_j$$

sive. They should only be synthesized in small quantities and should be treated with utmost care at all times. The copper metallacrown formed from anthranilic hydroxamic acid adopts a “sofa” configuration that is structurally reminiscent of porphyrin chemistry.²⁴ The best least-squares plane of the central copper(II) coordination sphere makes a 53° angle with the best least-squares plane of the phenyl ring carbons of the ligand. There are two distinct metallacrown structures in the crystal. One metallacrown has four methanol coordinated to the ring

(24) Scheidt, W. R.; Lee, Y. J. In *Recent Advances in the Stereochemistry of Metallotetrapyrroles*; Springer-Verlag: Berlin, 1987; Vol. 64, p 2.

Table 5. Selected Averaged Interatomic Bond Distances (Å) for the Generalized $[\text{Cu}^{\text{II}}(12\text{-MC}_{\text{Cu}(\text{II})\text{N}(\text{ligand})-4})]$ Structure Type: $[\text{Cu}^{\text{II}}(12\text{-MC}_{\text{Cu}(\text{II})\text{N}(\text{anba})-4})](\text{ClO}_4)_2$, **1b**, $(\text{TEA})_2[\text{Cu}^{\text{II}}(12\text{-MC}_{\text{Cu}(\text{II})\text{N}(\text{nba})-4})]$, **3**, $(\text{Na}(15\text{-C-5}))_2[\text{Cu}^{\text{II}}(12\text{-MC}_{\text{Cu}(\text{II})\text{N}(\text{shi})-4})]$, **4a**, and $(\text{TMA})_2[\text{Cu}^{\text{II}}(12\text{-MC}_{\text{Cu}(\text{II})\text{N}(\text{shi})-4})]$, **4b**

	1b	3	4a	4b
Cu(ring)–Cu(core)	3.262(2)	3.29(2)	3.282(2)	3.262(3)
Cu(ring)–Cu(ring)	4.611(1)	4.65(2)	4.561(1)	4.621(2)
Cu(core)–O _H	1.907(2)	1.905(5)	1.92(2)	1.871(3)
Cu(ring)–O _H	1.920(2)	1.930(5)	1.89(1)	1.900(3)
Cu–O _C	1.961(2)	1.971(2)	1.89(1)	1.967(3)
Cu–N _I	1.949(3)	1.953(7)	1.91(1)	1.842(2)
Cu–N _A	1.987(3)			
Cu–O _p		1.872(2)	1.85(2)	1.872(3)
Cu–O(sol)	2.373(3)	2.245(1)	2.35(2)	

copper(II) ions completing the square pyramidal geometry, shown in Figure 3. The other has two bound methanol on ring copper(II) ions related via the crystallographically imposed inversion center on which the core copper(II) ion resides. There is no significant difference in metrical parameters between the structures. The cavity size of **1b** is 0.66 Å allowing the core Cu(II) (Cu(II), 4-coordinate ionic radius = 0.57 Å)²³ to reside in the best least squares plane of the four metallacrown oxygens.

Description of the Structure of $(\text{TEA})_2[\text{Cu}^{\text{II}}(12\text{-MC}_{\text{Cu}(\text{II})\text{N}(\text{nba})-4})]$, **3.** The copper metallacrown formed with 3-hydroxy-2-naphthohydroxamic acid resembles a molecular disk in that the dimensions (excluding the coordinated DMF) are 1.8 nm × 1.8 nm × 0.4 nm.²⁵ Since the cavity size of this metallacrown is 0.69 Å, the central copper(II) (Cu(II), 6-coordinate ionic radius = 0.71 Å)²³ resides in the best least squares plane of the four metallacrown oxygens and has DMF bound in the axial positions. The change in coordination number of the central copper(II) does not affect the metrical parameters of the metallacrown ring significantly.

Description of the Structure of $(\text{Na}(15\text{-C-5}))_2[\text{Cu}^{\text{II}}(12\text{-MC}_{\text{Cu}(\text{II})\text{N}(\text{shi})-4})]$, **4a.** The copper metallacrown formed via salicylhydroxamic acid (H₃shi) and crystallized using (Na(15-C-5))⁺ has been examined and the structure solved to an *R* = 12.2%. This high residual was due to disorder in the organic crown ethers. The connectivity of the complex is similar to **3** where the central Cu(II) is five-coordinate and lies ≈0.15 Å above the best least squares plane of the metallacrown oxygens in a cavity of 0.66 Å. The overall configuration of the complex is domed, again structurally reminiscent of porphyrin chemistry.²⁴ However, this doming is probably due to interactions between the sodium cations and phenolate oxygen atoms of the metallacrown and crystal packing effects.

Description of the Structure of $(\text{TMA})_2[\text{Cu}^{\text{II}}(12\text{-MC}_{\text{Cu}(\text{II})\text{N}(\text{shi})-4})]$, **4b.** The copper(II) 12-metallacrown-4 formed with salicylhydroxamic acid as a tetramethylammonium salt is shown as a space-filling model in Figure 4. The metallacrown crystallizes as two independent molecules disordered about the inversion center on which the central copper resides. The occupancies of the two metallacrowns were refined to 55.2(1)% and 44.8(1)%. The metallacrown ring nitrogen positions and central copper(II) are coincidental in both metallacrowns. All the atoms of the two metallacrowns may be superimposed if one metallacrown is rotated by 180° along an axis parallel to the plane of the metallacrown and then rotated 52.7° along an axis perpendicular to the plane of the metallacrown. Similar to **3**, **4b** is a molecular disc of dimensions 1.4 nm × 1.4 nm × 0.4 nm,²⁵ mean deviation from plane = 0.15 Å. The topological similarities of the **4b** (1.4 nm × 1.4 nm × 0.4 nm) and copper-

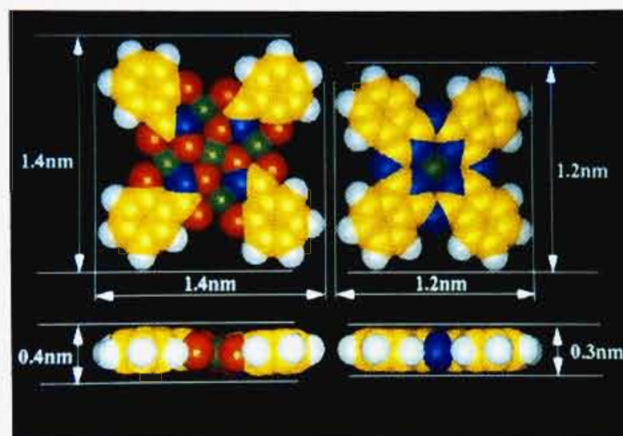


Figure 4. Corey–Pauling–Koltun (CPK) molecular models of $[\text{Cu}^{\text{II}}(12\text{-MC}_{\text{Cu}(\text{II})\text{N}(\text{shi})-4})]^{2-}$, **4b**, left, and copper(II) phthalocyanine,³⁵ right, illustrating the dimensions²³ and disk conformation of the metallacrown and the topological resemblance to copper(II) phthalocyanine. The copper(II) ions are shown in green, nitrogen atoms in blue, oxygen atoms in red, carbon atoms in yellow and hydrogen atoms in white. The CPK scale is 1.0.

(II) phthalocyanine (1.2 nm × 1.2 nm × 0.3 nm)³⁵ are illustrated in Figure 4. The cavity size of this metallacrown is 0.61 Å allowing the central copper(II) (Cu(II), 4-coordinate ionic radius = 0.57 Å)²³ to reside in the best least-squares plane of the four metallacrown oxygens.

Metallacrown Formation and Solution Integrity Investigations by UV–Vis. Solution stability of the metallacrowns is a fundamental property for the proposed applications of metallacrowns. UV–vis titrations (either of metal solutions into ligand solutions or ligand solutions into metal solutions) were undertaken both to determine the extent of solution integrity and to provide insight into metallacrown formation. Addition of 0.1 equiv aliquots of salicylhydroxamic acid to 1 mM Cu(OAc)₂ in DMF in the presence of excess sodium acetate (20 mM) was followed by UV–vis spectroscopy. As the first 0.5 equiv of H₃shi was added, the ligand field band of the copper(II) ions blue shifted and an isosbestic point was observed at λ = 638 nm. The presence of the isosbestic point, as shown in Figure 5, implies formation of a Cu₂L species in solution, illustrated in Scheme 1. Beyond 0.5 equiv, the isosbestic behavior is lost and at 0.8 equiv the visible spectrum of the metallacrown, **4**, (λ_{max} = 618 nm, ε = 178 M⁻¹ cm⁻¹ per Cu(II)) is maximized. Addition of excess H₃shi to the reaction mixture changes neither the position nor intensity of the d–d absorption band. At high [shi³⁻]/[Cu(II)] ratios, the dissociation of the metallacrown into mononuclear species, i.e. CuL₂, was not observed. We conclude from these results that the metallacrown structure is present in solution, and that the presence of excess ligand and acetate do not adversely affect the $[\text{Cu}^{\text{II}}(12\text{-MC}_{\text{Cu}(\text{II})\text{N}-4})]$ motif.

The addition of Cu(OAc)₂ to H₃shi in DMF in the presence of excess sodium acetate was also followed by UV–vis spectroscopy. The titration curve is shown in Figure 6 and is representative of all the ligands in this study. An increase in the absorbance at 618 nm was observed with a metal to ligand endpoint ratio of 1.2:1, consistent with 12-MC-4 formation. The spectrum at the metal to ligand ratio of 5:4 was identical to the spectrum of an authentic crystalline sample of **4a** (λ_{max} = 618 nm, ε = 178 M⁻¹ cm⁻¹ per Cu(II)). Addition of excess metal, up to 3.5 equiv per ligand, does not alter the copper(II) ligand field band, but does add a shoulder at 700 nm consistent with uncomplexed Cu(II) in solution. These observations are

Table 6. Range of Selected Interatomic Bond Angles (deg) for the Generalized $[\text{Cu}^{\text{II}}(12\text{-MC}_{\text{Cu}(\text{II})\text{N}(\text{ligand})-4})]$ Structure Type: $[\text{Cu}^{\text{II}}(12\text{-MC}_{\text{Cu}(\text{II})\text{N}(\text{anha})-4})(\text{ClO}_4)_2]$, **1b**, $(\text{TEA})_2[\text{Cu}^{\text{II}}(12\text{-MC}_{\text{Cu}(\text{II})\text{N}(\text{nha})-4})]$, **3**, $(\text{Na}^+(15\text{-C-5}))_2[\text{Cu}^{\text{II}}(12\text{-MC}_{\text{Cu}(\text{II})\text{N}(\text{shi})-4})]$, **4a**, and $(\text{TMA})_2[\text{Cu}^{\text{II}}(12\text{-MC}_{\text{Cu}(\text{II})\text{N}(\text{shi})-4})]$, **4b**

	1b	3	4a	4b
$\text{O}_\text{H}-\text{Cu}_\text{R}-\text{O}_\text{C}$	80.38(8)–81.76(8)	79.2(1)–80.5(2)	80.4(6)–81.5(5)	80.13(4)–80.63(3)
$\text{O}_\text{H}-\text{Cu}_\text{R}-\text{N}_\text{I}$	89.01(9)–90.48(9)	86.6(2)–90.2(3)	89.3(5)–93.1(5)	88.61(11)–90.10(2)
$\text{N}_\text{I}-\text{Cu}_\text{R}-\text{N}_\text{A}$	88.0(1)–90.7(1)			
$\text{N}_\text{A}-\text{Cu}_\text{R}-\text{O}_\text{C}$	98.2(1)–101.1(1)			
$\text{N}_\text{I}-\text{Cu}_\text{R}-\text{O}_\text{P}$		92.1(2)–92.6(2)	91.8(5)–94.7(5)	91.72(12)–92.68(3)
$\text{O}_\text{P}-\text{Cu}_\text{R}-\text{O}_\text{C}$		96.9(1)–98.9(1)	91.9(6)–96.5(5)	97.58(14)–98.95(14)
$\text{Cu}_\text{R}-\text{O}_\text{O}-\text{Cu}_\text{C}$	114.7(1)–120.9(1)	110.8(2)–120.9(4)	116.2(6)–121.4(7)	117.5(2)–120.4(2)
$\text{O}_\text{H}-\text{Cu}_\text{C}-\text{O}_\text{H}$	88.40(9)–91.60(9)	89.2(2)–90.8(2)	86.5(5)–92.6(5)	88.90(14)–91.10(14)

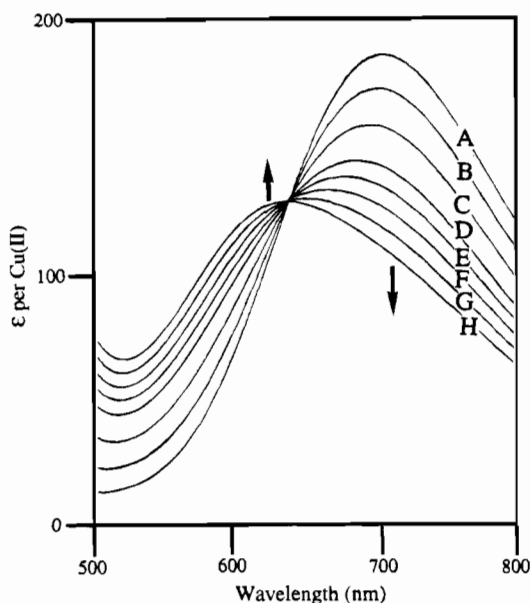


Figure 5. UV-vis spectra of the titration of 0.0–0.5 equiv of H_3shi into a DMF solution 1 mM in $\text{Cu}(\text{OAc})_2$ and 20 mM in NaOAc . Key: A = 0.0 equiv; B = 0.10 equiv; C = 0.20 equiv; D = 0.30 equiv; E = 0.35 equiv; F = 0.40 equiv; G = 0.45 equiv; H = 0.50 equiv. The isosbestic point at $\lambda = 638$ nm supports the formation of the proposed Cu_2L intermediate in the metallacrown formation.

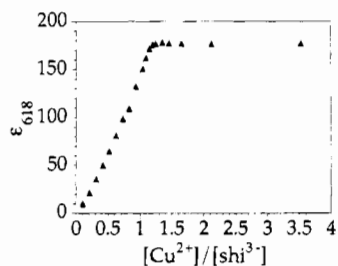


Figure 6. UV-vis titration curve of the addition of 0.0–3.5 equiv of $\text{Cu}(\text{OAc})_2$ into 1 mM H_3shi and 20 mM NaOAc in DMF.

consistent with the stability of the copper(II) 12-metallacrown-4 in DMF even in the presence of excess metal. The $[\text{Cu}^{\text{II}}(12\text{-MC}_{\text{Cu}(\text{II})\text{N}-4})]$ retains its structure in solution in the presence of excess $\text{Cu}(\text{II})$ and base.

Solution Speciation Using Mass Spectrometry. The solution integrity of metallacrowns and their solution dynamics are two of the most fundamentally important properties that are desirable for utilization of the metallacrowns as platforms for supramolecular architecture. The solution speciation of the copper metallacrowns was addressed using solution mass spectrometry. When dissolved in DMF in a 3-nitrobenzyl alcohol matrix, the copper metallacrowns **1b**, **3**, and **4a** give strong molecular ions in the FAB-MS. We have found that **4b** did not give a satisfactory molecular ion in the FAB-MS most likely due to poor solubility in the matrix coupled with the poor volatility of these complexes. The addition of the organic crown

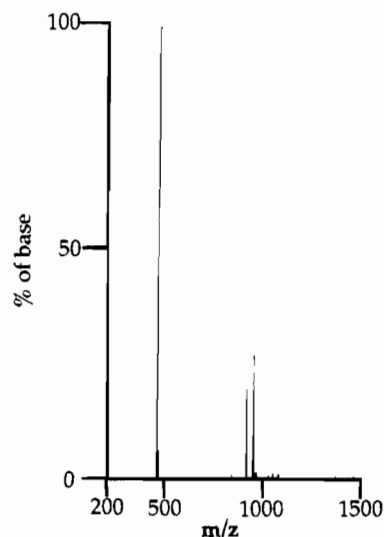


Figure 7. ESI-MS(+) of $[\text{Cu}^{\text{II}}(12\text{-MC}_{\text{Cu}(\text{II})\text{N}(\text{paha})-4})]^{2+}$, **2**, from MeOH. The peak at m/z 918 (22% of base) is the molecular ion. The peak at m/z 459 (base) is the intact ion. The m/z 953 peak (30% of base) corresponds to association of one chloride anion with the molecular ion.

ether, 15-C-5, dramatically increases the solubility of **4a** in MeOH, with respect to **4b**, and allows observation of the molecular ion in the FAB-MS.

In order to circumvent the need to prepare copper metallacrowns with various counterions we began utilizing electrospray ionization mass spectrometry (ESI-MS).^{26–29} This soft ionization technique allows for detection of all ions in solution.²⁶ Since the copper metallacrowns in this study are either dicationic or dianionic and are soluble in either MeOH or CH_3CN , molecular ions are readily observed in the ESI-MS. All the reported $[\text{Cu}^{\text{II}}(12\text{-MC}_{\text{Cu}(\text{II})\text{N}(\text{ligand})-4})]$ complexes show intact ions²⁷ and molecular ions in the ESI-MS. A typical ESI-MS of $[\text{Cu}^{\text{II}}(12\text{-MC}_{\text{Cu}(\text{II})\text{N}(\text{paha})-4})]^{2+}$, **2**, is shown in Figure 7. Both the molecular ion, $\text{M}^+ = m/z$ 918, and the intact ion, $\text{M}^{2+} = m/z$ 459, are readily observed. The m/z 953 peak corresponds to the association of a single chloride anion with the metallacrown, i.e. $\{[\text{Cu}^{\text{II}}(12\text{-MC}_{\text{Cu}(\text{II})\text{N}(\text{anha})-4})(\text{Cl})]\}^+$.

Ligand Exchange between Metallacrowns. Colton and co-workers have recently begun probing solution dynamics with ESI-MS as it allows for one to probe mass distributions at a

(25) Length and width dimensions were measured using aromatic ring hydrogen atoms. Height of the metallacrown and phthalocyanine were taken as the van der Waals diameter of the atom with the greatest deviation from the best least squares plane of the atoms plus double the maximum deviation from the plane.

(26) Kebarie, P.; Tang, L. *Anal. Chem.* **1993**, *65*, 927A.

(27) Price, P. J. *J. Am. Soc. Mass Spectrom.* **1991**, *2*, 336.

(28) Katta, V.; Chowdhury, S. K.; Chait, B. T. *J. Am. Chem. Soc.* **1990**, *112*, 5348.

(29) Smith, R. D.; Loo, J. A.; Edmonds, C. G.; Barinaga, C. J.; Udseth, H. R. *Anal. Chem.* **1990**, 882.

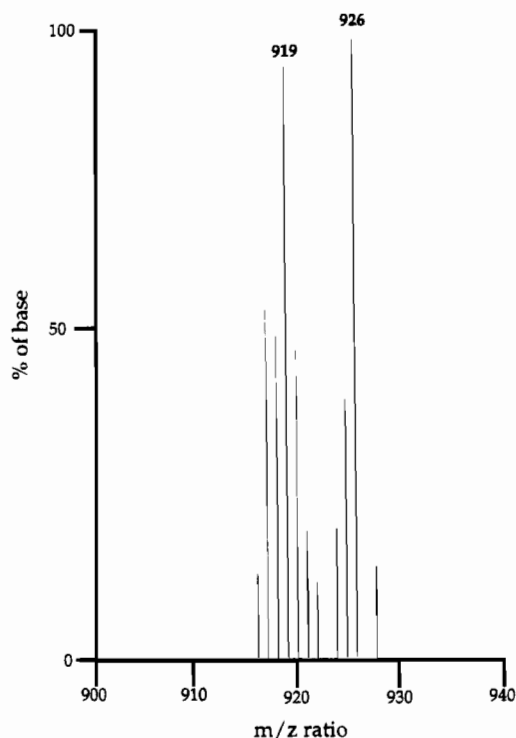
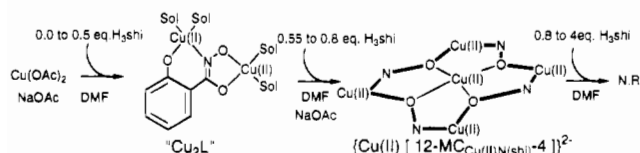


Figure 8. ESI-MS(–) of a 1:1 mixture of $[\text{Cu}^{\text{II}}(12\text{-MC}_{\text{Cu}(\text{II})\text{N}(\text{shi})-4})]^{2-}$, **4b**, and $[\text{Cu}^{\text{II}}(12\text{-MC}_{\text{Cu}(\text{II})\text{N}(\text{d2shi})-4})]^{2-}$, **5b**, after 6 h in CH_3CN .

Scheme 1



moment in time.^{30,31} The copper metallacrowns synthesized from protio-, 5-deuterio-, and 3,5-dideuteriosalicylhydroxamic acid allow for observation of ligand exchange between thermodynamically equivalent copper metallacrowns. The ESI-MS of **4b** and **5b** were recorded separately and then in a 1:1 mixture. Both molecular ions, at m/z 919 for **4b** and m/z 926 for **5b**, are resolved in the initial mass spectrum. When a second mass spectrum is recorded on the same sample 6 h later, there is no observable ligand mixing between the metallacrowns, as shown in Figure 8. The lack of thermodynamic penalties for the ligand mixing and the lack of observable exchange strongly demonstrate the solution integrity of the shi³⁻ based copper metallacrown, **4b**, in CH_3CN .

Further evidence demonstrating that ligand exchange does not occur with $[\text{Cu}^{\text{II}}(12\text{-MC}_{\text{Cu}(\text{II})\text{N}-4})]$ is obtained by monitoring exchange directly via ¹H NMR using $[9\text{-MC}_{\text{V}(\text{V})\text{O}(\text{N}(\text{nha})-3)}$, **11**, which is kinetically labile in methanol⁹ with a measured ligand exchange rate of $0.31 \pm 0.02 \text{ h}^{-1}$. Due to the 1:1 metal to ligand ratio in **11** and its inability to sequester metal ions in its cavity,⁹ it is ideal for ligand exchange experiments. The ligand exchange rates of **1a** and **4a** were evaluated by mixing equimolar solutions of each with $[9\text{-MC}_{\text{V}(\text{V})\text{O}(\text{N}(\text{nha})-3)}$ in methanol. Both **1a** and **4a** showed no signs of ligand exchange in the ¹H NMR after 24 h. With the established lability of the vanadium metallacrown, this proves that these two copper 12-MC-4's are kinetically inert to ligand exchange. Similarly, FAB-MS of

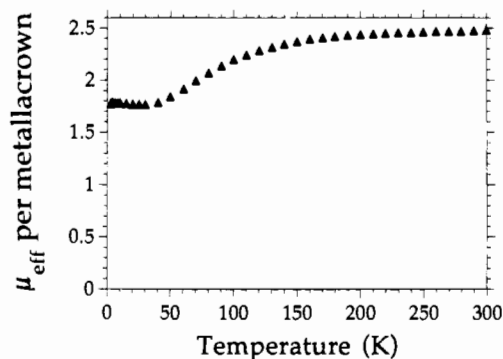


Figure 9. Magnetic moment of **1a** in a magnetic field of 10 kOe between 2.5 and 300 K.

methanol solutions of 1:1 ratios of **1a** or **4** with **11** provided mass peaks only for the starting complexes. As a control, mixed-ligand complexes were prepared directly and showed the expected mass peaks for mixed-ligand complexes.

Magnetic Susceptibility Measurements. The room temperature solid state and solution magnetic moments and the solid state magnetic moments at 4.2 K for all the $[\text{Cu}^{\text{II}}(12\text{-MC}_{\text{Cu}(\text{II})\text{N}(\text{ligand})-4})]$ complexes are given in Table 7. The temperature dependence of the magnetic moment of **1a** is illustrated in Figure 9 and is representative of all the metallacrowns in this study. The solid state room temperature value, $2.48 \mu_{\text{B}}$, is considerably lower than the $5.91 \mu_{\text{B}}$ predicted for an $S = 5/2$ system. The magnetic moment of **1a** at 4.2 K, $1.79 \mu_{\text{B}}$, support an $S = 1/2$ ground state, consistent with antiferromagnetic coupling of the copper(II) ions. This antiferromagnetic coupling allows four of the copper(II) ions to be paired at 4.2 K, yielding a doublet ground state. The complex is EPR silent at 77 K, but at 6 K has an isotropic EPR signal at $g \approx 2.0$, which is consistent with a doublet ground state. The lack of an EPR signal at 77 K also corroborates the previous observation of their solution integrity, as any mononuclear copper(II) formed during metallacrown dissociation processes is expected to be EPR active.³² The room temperature solution susceptibilities, measured in DMF using Evans' method,^{33,34} are comparable to their solid state moments consistent with metallacrown integrity in DMF and weak intracluster exchange in the solid.

Discussion

The structural characterization of four $[\text{Cu}^{\text{II}}(12\text{-MC}-4)]$'s and the synthesis of nine additional $[\text{Cu}^{\text{II}}(12\text{-MC}-4)]$'s clearly demonstrates the versatility of the metallacrown analogy for the rational synthesis of polynuclear transition metal complexes. Each of the structurally characterized $[\text{Cu}^{\text{II}}(12\text{-MC}-4)]$'s retain the high yield, one-step metallacrown synthesis resulting in a $[\text{Cu}^{\text{II}}(12\text{-MC}-4)]$ whose metrical parameters vary little with choice of supporting ligand. The ligand variability⁹ of the 12-MC-4 and 9-MC-3 structural motifs provide strong evidence of the metallacrown analogy as a powerful synthetic protocol. Unlike previously reported metallacrowns, neutral metallacrown rings result from using anha^{2-} or paha^{2-} as the supporting ligands with a divalent metal. Additionally, the divalent ligands provide alterations in the metallacrown ring metal ion donor sets which changes the electronic spectra of the metallacrowns as shown in Table 8. When shi³⁻ and any of its derivatives provide the organic scaffolding, the resulting metallacrowns are

(30) Colton, R.; James, B. D.; Potter, I. D.; Traeger, J. C. *Inorg. Chem.* **1993**, *32*, 2626.

(31) Colton, R.; Tedesco, V.; Traeger, J. C. *Inorg. Chem.* **1992**, *31*, 3865–3866.

(32) Addition of HClO_4 to the EPR sample results in a EPR spectrum consistent with uncomplexed Cu(II) in solution.

(33) Evans, D. F. *J. Chem. Soc.* **1959**, 2003.

(34) Bartle, K. D.; Dale, B. J.; Jones, D. W.; Maricic, J. J. *Magn. Reson.* **1973**, *12*, 286.

Table 7. Magnetic Moments of [Cu^{II}(12-MC_{Cu(II)N(ligand)}-4)] (μ_B /Complex)

compd	solution (300 K) ^a	solid (300 K)	solid (4 K)
1a	2.56	2.48	1.79
2	2.33	2.54	1.74
3	2.37	2.45	1.78
4b	2.59	2.48	1.77
5b	2.59	2.48	1.77
6	2.40	2.46	1.76
7	2.48	2.58	1.75
8	2.42	2.49	1.75
9	2.47	2.66	1.73
10	2.43	2.40	1.73

^a In DMF.**Table 8.** UV-Vis Parameters for [Cu^{II}(12-MC_{Cu(II)N(ligand)}-4)] Derivatives

complex	λ_{\max} (ϵ^a)	
	acetonitrile	DMF
1a	600 (107)	612 (109)
2	623 (98)	623 (66)
3	616 (237)	620 (210)
4a,b	615 (189)	618 (178)
5a,b	615 (189)	618 (178)
6	615 (196)	615 (190)
7	615 (191) ^b	616 (196)
8	616 (188)	615 (192)
9	616 (181) ^b	617 (195)
10	617 (182) ^b	617 (176)

^a Extinction coefficient in M⁻¹ cm⁻¹ per copper(II). ^b Dissolution was accomplished by addition of 2 equiv of 15-C-5 per Na⁺ (**7**) or K⁺ (**9** and **10**).

the first examples containing formally charged, i.e. 4-, metallacrown rings. This charge on the metallacrown ring does not hinder metallacrown formation. Addition of peripheral hydroxyl groups to the metallacrowns via 4-ohshi³⁻ and 5-ohshi³⁻ provide evidence that further ligand modification may be made.

A wide variety of analytical techniques have been employed for the evaluation of the solution integrity of the [Cu^{II}(12-MC_{Cu(II)N(ligand)}-4)]'s presented herein. UV-vis titrations provide evidence that the metallacrowns studied retain their structure in DMF even under conditions of excess Cu(II) or excess ligand. These titrations also provide insight into the process of metallacrown formation. The existence of an isosbestic point ($\lambda = 632$ nm) up to 0.5 equiv in the titration of H₃shi into Cu(OAc)₂/NaOAc in DMF supports the Cu₂L intermediate in metallacrown formation, shown in Scheme 1. Addition of additional ligand, up to 0.8 equiv, results in a UV-vis spectrum consistent with metallacrown formation.

Mass spectrometry via electrospray ionization (ESI-MS) or fast atom bombardment (FAB-MS) confirmed the integrity of the [Cu^{II}(12-MC-4)]'s in solution. All of the presented metallacrowns provide mass spectra from solution consistent with retention of metallacrown structure. Since ESI-MS can provide kinetic information about ligand exchange reactions, we utilized the deuterated analogs of **4b** to investigate the solution dynamics of the metallacrowns in a reaction lacking thermodynamic penalties. The ESI-MS spectrum of a 1:1 mixture of **4b** and **5b** in CH₃CN after 6 h provides no evidence for ligand exchange, as shown in Figure 8. This mass spectrum emphatically demonstrates the integrity of the copper metallacrowns in CH₃CN. Additionally, the ligand exchange kinetics of **1b** and **4a** were investigated in methanol using the labile [9-MC-(V(V)O)N(nha)-3], **11**. Reactions of a 1:1 mixture of the vanadium metallacrown and either **1b** or **4a** showed no observable signs of ligand exchange via ¹H NMR after 24 h. This result confirms

the already daunting evidence for the integrity of these metallacrowns in solution.

EPR studies showed the [Cu^{II}(12-MC-4)]'s to be EPR silent at 77 K and EPR active at 6 K with an isotropic signal at $g \approx 2.0$. These results are consistent with weakly antiferromagnetically coupled Cu(II) ions. Solid state variable temperature magnetic moment measurements confirm the existence of an $S = 1/2$ ground state.

The peripheral modifications of shi³⁻ provide evidence that metallacrowns may be used for supramolecular design. The molecular dimensions of the metallacrowns, **3** and **4b**, (1.8 nm × 1.8 nm × 0.4 nm and 1.4 nm × 1.4 nm × 0.4 nm, respectively) make them true nanoparticles. As illustrated in Figure 4, the topology of **4b** resembles copper(II) phthalocyanine³⁵ which has slightly smaller molecular dimensions of 1.2 nm × 1.2 nm × 0.3 nm. Functionalization of copper(II) phthalocyanine with alkyloxy chains has yielded discotic columnar mesophases.^{18,36-38} The remarkable shape similarity suggests that the addition of peripheral alkyl and alkyloxy functionalities to the disk shaped copper(II) metallacrowns, represented in principle by **7**, **9** and **10**, will provide discotic metallomesogens that contain metal clusters that are more highly paramagnetic than simple metallophthalocyanines. Once synthesized, a discotic copper(II) metallacrown would have a magnetic moment of $\approx 2.5 \mu_B$ at room temperature, compared to $\mu_{\text{eff}} \approx 1.7 \mu_B$ for copper(II) phthalocyanine.³⁹ Furthermore, the related [Li^I(12-MC_{Mn(III)N(shi)}-4)]⁺, exhibits a magnetic moment of $9.8 \mu_B$ ⁴⁰ compared with the diamagnetic lithium(I) phthalocyanine,⁴¹ and the [Mn^{II}(12-MC_{Mn(III)N(shi)}-4)]²⁺ ($\mu_{\text{eff}} = 13.8 \mu_B$) more than triples the paramagnetism per unit volume compared to manganese(II) phthalocyanine ($\mu_{\text{eff}} \approx 4.4 \mu_B$).⁴² These observations suggest that workers armed with these new materials may significantly enhance the magnetic properties of mesogenic phases.

Acknowledgment. We greatly appreciate the A. P. Sloan Foundation for support of this work. The authors would like to thank Ann J. Stemmler for valued discussions. B.R.G. would like to thank the Department of Chemistry, University of Michigan, for a Smeaton Fellowship.

Supplementary Material Available: Tables S1-S20 provide a complete crystallographic summary, anisotropic thermal parameters of all non-hydrogen atoms, fractional atomic positions for hydrogen atoms, a complete set of bond distances, and a complete set of bond angles for **1b**, **3**, **4a**, and **4b**. Figures S1 and S2 provide the complete numbering scheme for all atoms of both molecules of **1b**. Figure S3 gives a complete numbering scheme for all atoms of **3**. Figure S4 provides a complete numbering scheme for all atoms of **4a**. Figure S5 and S6 provide complete numbering scheme for all atoms of **4b**. Figures S7-S15 provide variable temperature magnetic moments for compounds **2-10** (66 pages). Ordering information is given on any current masthead page.

- (35) Brown, C. J. *J. Chem. Soc. A* **1968**, 2488.
 (36) Piechocki, C.; Simon, J.; Skoulios, A.; Guillon, D.; Weber, P. *J. Am. Chem. Soc.* **1982**, *104*, 5245.
 (37) Cook, M. J.; Daniel, M. F.; Harrison, K. J.; McKeown, N. B.; Thomson, A. J. *J. Chem. Soc., Chem. Commun.* **1987**, 1086.
 (38) Piechocki, P.; Simon, J. *Nouv. J. Chem.* **1985**, *9*, 159.
 (39) Gibson, J. F.; Ingram, D. J. E.; Schonland, D. *Discuss. Faraday Soc.* **1958**, *26*, 72.
 (40) Gibney, B. R.; Wang, H.; Stemmler, A. J.; Kampf, J. W.; Pecoraro, V. L. Presented at the 207th National Meeting of the American Chemical Society, San Diego, CA, 1994; Poster No. 358.
 (41) Belarbi, Z.; Sirlin, C.; Simon, J.; Andre, J.-J. *J. Phys. Chem.* **1989**, *93*, 8105.
 (42) Lever, A. B. P. *J. Chem. Soc.* **1965**, 1821.